Atmospheric histories and growth trends of C_4F_{10}, C_5F_{12}, C_6F_{14}, C_7F_{16} and C_8F_{18}[*]

Diane J. Ivy, Tim Arnold, Christina M. Harth, L. Paul Steele, Jens Mühle, Matthew Rigby, Peter K. Salameh, Michael Leist, Paul B. Krummel, Paul J. Fraser, Ray F. Weiss and Ronald G. Prinn

MIT JOINT PROGRAM

SCIENCE

POLICY

GLOBAL CHANGE

MIT JOINT PROGRAM ON THE SCIENCE AND POLICY of GLOBAL CHANGE

The MIT Joint Program on the Science and Policy of Global Change combines cutting-edge scientific research with independent policy analysis to provide a solid foundation for the public and private decisions needed to mitigate and adapt to unavoidable global environmental changes. Being data-driven, the Program uses extensive Earth system and economic data and models to produce quantitative analysis and predictions of the risks of climate change and the challenges of limiting human influence on the environment—essential knowledge for the international dialogue toward a global response to climate change.

To this end, the Program brings together an interdisciplinary group from two established MIT research centers: the Center for Global Change Science (CGCS) and the Center for Energy and Environmental Policy Research (CEEPR). These two centers—along with collaborators from the Marine Biology Laboratory (MBL) at Woods Hole and short- and long-term visitors—provide the united vision needed to solve global challenges.

At the heart of much of the Program's work lies MIT's Integrated Global System Model. Through this integrated model, the Program seeks to: discover new interactions among natural and human climate system components; objectively assess uncertainty in economic and climate projections; critically and quantitatively analyze environmental management and policy proposals; understand complex connections among the many forces that will shape our future; and improve methods to model, monitor and verify greenhouse gas emissions and climatic impacts.

This reprint is one of a series intended to communicate research results and improve public understanding of global environment and energy challenges, thereby contributing to informed debate about climate change and the economic and social implications of policy alternatives.

Ronald G. Prinn and John M. Reilly,
Program Co-Directors

For more information, contact the Program office:

MIT Joint Program on the Science and Policy of Global Change
Postal Address:
Massachusetts Institute of Technology
77 Massachusetts Avenue, E19-411
Cambridge, MA 02139 (USA)
Location:
Building E19, Room 411
400 Main Street, Cambridge
Access:
Tel: (617) 253-7492
Fax: (617) 253-9845
Email: ***globalchange@mit.edu***
Website: ***http://globalchange.mit.edu/***

Atmospheric Chemistry and Physics

Atmospheric histories and growth trends of C_4F_{10}, C_5F_{12}, C_6F_{14}, C_7F_{16} and C_8F_{18}

D. J. Ivy[1], T. Arnold[2], C. M. Harth[2], L. P. Steele[3], J. Mühle[2], M. Rigby[1,*], P. K. Salameh[2], M. Leist[3,**], P. B. Krummel[3], P. J. Fraser[3], R. F. Weiss[2], and R. G. Prinn[1]

[1]Center for Global Change Science, Massachusetts Institute of Technology, Cambridge, Massachusetts, USA
[2]Scripps Institution of Oceanography, Univ. of California San Diego, La Jolla, California, USA
[3]Centre for Australian Weather and Climate Research, CSIRO Marine and Atmospheric Research, Aspendale, Victoria, Australia
[*]now at: Atmospheric Chemistry Research Group, University of Bristol, Bristol, UK
[**]now at: Defence Science and Technology Organisation, Department of Defence, Melbourne, Victoria, Australia

Correspondence to: D. J. Ivy (divy@mit.edu)

Abstract. Atmospheric observations and trends are presented for the high molecular weight perfluorocarbons (PFCs): decafluorobutane (C_4F_{10}), dodecafluoropentane (C_5F_{12}), tetradecafluorohexane (C_6F_{14}), hexadecafluoroheptane (C_7F_{16}) and octadecafluorooctane (C_8F_{18}). Their atmospheric histories are based on measurements of 36 Northern Hemisphere and 46 Southern Hemisphere archived air samples collected between 1973 to 2011 using the Advanced Global Atmospheric Gases Experiment (AGAGE) "Medusa" preconcentration gas chromatography-mass spectrometry systems. A new calibration scale was prepared for each PFC, with estimated accuracies of 6.8 % for C_4F_{10}, 7.8 % for C_5F_{12}, 4.0 % for C_6F_{14}, 6.6 % for C_7F_{16} and 7.9 % for C_8F_{18}. Based on our observations the 2011 globally averaged dry air mole fractions of these heavy PFCs are: 0.17 parts-per-trillion (ppt, i.e., parts per 10^{12}) for C_4F_{10}, 0.12 ppt for C_5F_{12}, 0.27 ppt for C_6F_{14}, 0.12 ppt for C_7F_{16} and 0.09 ppt for C_8F_{18}. These atmospheric mole fractions combine to contribute to a global average radiative forcing of $0.35\,\mathrm{mW\,m^{-2}}$, which is 6 % of the total anthropogenic PFC radiative forcing (Montzka and Reimann, 2011; Oram et al., 2012). The growth rates of the heavy perfluorocarbons were largest in the late 1990s peaking at 6.2 parts per quadrillion (ppq, i.e., parts per 10^{15}) per year (yr) for C_4F_{10}, at $5.0\,\mathrm{ppq\,yr^{-1}}$ for C_5F_{12} and $16.6\,\mathrm{ppq\,yr^{-1}}$ for C_6F_{14} and in the early 1990s for C_7F_{16} at $4.7\,\mathrm{ppq\,yr^{-1}}$ and in the mid 1990s for C_8F_{18} at $4.8\,\mathrm{ppq\,yr^{-1}}$. The 2011 globally averaged mean atmospheric growth rates of these PFCs are subsequently lower at $2.2\,\mathrm{ppq\,yr^{-1}}$ for C_4F_{10}, $1.4\,\mathrm{ppq\,yr^{-1}}$ for C_5F_{12}, $5.0\,\mathrm{ppq\,yr^{-1}}$ for C_6F_{14}, $3.4\,\mathrm{ppq\,yr^{-1}}$ for C_7F_{16} and $0.9\,\mathrm{ppq\,yr^{-1}}$ for C_8F_{18}. The more recent slowdown in the growth rates suggests that emissions are declining as compared to the 1980s and 1990s.

1 Introduction

Perfluorocarbons (PFCs) are powerful greenhouse gases regulated under the Kyoto Protocol to the United Nations Framework Convention on Climate Change (UNFCCC). Due to their long lifetimes and strong absorption in the infrared, PFCs are considered to have a permanent effect on the Earth's radiative budget and have global warming potentials (GWPs) 3 to 4 orders of magnitude higher than that of carbon dioxide (CO_2), see Table 1, (Forster et al., 2007). Observations and atmospheric-observation-based emission estimates are available for carbon tetrafluoride (CF_4), hexafluoroethane (C_2F_6), octafluoropropane (C_3F_8) and octafluorocyclobutane (c-C_4F_8) (Mühle et al., 2010; Oram et al., 2012; Saito et al., 2010). CF_4 is the most abundant PFC and has a significant natural abundance (Deeds et al., 2008; Harnisch et al., 1996a,b; Mühle et al., 2010). The predominant anthropogenic emissions of these lower molecular weight PFCs are from the production of aluminum, usage in the

Table 1. Lifetimes, Radiative Efficiencies and Global Warming Potentials of Perfluorocarbons.

Species	Lifetime [yr]	Radiative Efficiency $[\mathrm{W\,m^{-2}\,ppb^{-1}}]$	Global Warming Potential (GWP) 20-yr horizon	100-yr horizon	500-yr horizon	Reference
CF_4	50 000	0.10	5210	7390	11 200	Forster et al. (2007)
C_2F_6	10 000	0.26	8630	12 200	18 200	Forster et al. (2007)
C_3F_8	2600	0.26	6310	8830	12 500	Forster et al. (2007)
$c\text{-}C_4F_8$	3200	0.32	7310	10300	14 700	Forster et al. (2007)
C_4F_{10}	2600	0.33	6330	8860	12 500	Forster et al. (2007)
C_5F_{12}	4100	0.41	6510	9160	13 300	Forster et al. (2007)
C_6F_{14}	3200	0.49	6600	9300	13 300	Forster et al. (2007)
C_7F_{16}	(3000)*	0.45	–	–	–	Bravo et al. (2010)
C_7F_{16}	(3000)*	0.48	–	–	–	Ivy et al. (2012)
C_8F_{18}	(3000)*	0.50	5280	7390	10 500	Bravo et al. (2010)
C_8F_{18}	(3000)*	0.57	–	–	–	Ivy et al. (2012)
$C_{10}F_{18}$	>1000	0.56	>5500	>7500	>9500	Shine et al. (2005)

* Lifetimes in parentheses have not been measured; a lifetime of 3000 yr was chosen as it is similar to that of C_6F_{14}.

semiconductor industry and as refrigerants (Mühle et al., 2010; Oram et al., 2012). Both the aluminum and semiconductor industries have made efforts to reduce emissions of the lower molecular weight PFCs to the atmosphere, although global bottom-up inventories show discrepancies with atmospheric-observation-based ("top-down") emission estimates (Mühle et al., 2010; International Aluminium Institute, 2011; Semiconductor Industry Association, 2001; World Semiconductor Council, 2005).

Currently, there is much less information available on the higher molecular weight PFCs: decafluorobutane (C_4F_{10}), dodecafluoropentane (C_5F_{12}), tetradecafluorohexane (C_6F_{14}), hexadecafluoroheptane (C_7F_{16}) and octadecafluorooctane (C_8F_{18}). These PFCs have emission sources similar to other halocarbons, e.g. their usage as refrigerants, solvents, fire suppressants and foam blowing agents; they were initially suggested as replacements for ozone depleting substances (ODS) that are regulated under the Montreal Protocol (UNEP Technology and Economic Assessment Panel, 1999; Tsai, 2009). Moreover, C_5F_{12}-C_8F_{18} (liquids at room temperature), have a first-of-a-kind emission source for fluorinated compounds from their use as heat transfer fluids in the semiconductor industry (where previously deionized water and a mixture of glycol and deionized water were used) (Tsai, 2009; Tuma and Tousignant, 2001). The main sink for the PFCs is photolysis by Lyman-α radiation and a minor destruction pathway is reaction with $O(^1D)$ (Ravishankara et al., 1993). In this study, atmospheric observations of C_4F_{10}, C_5F_{12}, C_6F_{14}, C_7F_{16} and C_8F_{18} are presented based on measurements of Northern Hemisphere (NH) and Southern Hemisphere (SH) archived air samples. These samples cover a 39-year period, from 1973 to 2011, and include 36 NH and 46 SH separate samples. Additionally, long-term growth trends are presented based on the atmospheric histories for the high molecular weight PFCs.

2   Experimental methods

2.1   Instrumentation

The cryogenic preconcentration gas chromatography-mass spectrometry (GC-MS: Agilent 6890-5973/5975) "Medusa" systems (Arnold et al., 2012; Miller et al., 2008) were used to measure the heavy PFC mole fractions in archived air samples at the Scripps Institution of Oceanography (SIO), University of California, San Diego (San Diego, CA) and at the Commonwealth Scientific and Industrial Research Organisation (CSIRO), Division of Marine and Atmospheric Research (CMAR, Aspendale, Australia). These instruments are part of the Advanced Global Atmospheric Gases Experiment (AGAGE) network. For each measurement, the condensables in a 2-l air sample are preconcentrated onto a micro-trap and then cyrofocused onto a second micro-trap (both micro-traps are initially held at −160 °C and subsequently heated for desorption) before injection onto a capillary column. Currently, the Medusa systems in AGAGE use a CP-PoraBOND Q fused silica PLOT column (25 m, 0.32 mm ID, 5 μm, Agilent Technologies) as the main column for separation of all analytes (except CF_4 and NF_3) (see Arnold et al. (2012); Miller et al. (2008) for details). However for the measurements at CSIRO, the Medusa was fitted with a GS-GasPro column (60 m, 0.32 mm ID, Agilent Technologies) as the main column, which had improved separation for these analytes. To maximize the measurements' precisions, the quadrupole MS was operated in selective ion mode (SIM). Additionally, only a select number of species were measured in this experiment, as compared to the more than 50 species typically measured as part of the AGAGE network, to minimize the number of acquired ions and further improve sample precisions. Each sample measurement was bracketed by a reference gas analysis, allowing for correction of short-term instrumental drift (Prinn et al., 2000). A small

Table 2. Retention Times, Target and Qualifier Mass-to-Charge Ratios, Standard Precisions and Detection Limits for C_4F_{10}, C_5F_{12}, C_6F_{14}, C_7F_{16} and C_8F_{18}.*

Species	Main Column	MS	Retention Time [s]	Target [m/z]	Qualifier 1 [m/z]	Qualifier 2 [m/z]	Standard Precision [ppt]	Detection Limit [ppt]
C_3F_8	PoraBOND	5975	510					
	GasPro	5973	705					
$CHClF_2$ [HCFC-22]	PoraBOND	5975	539					
	GasPro	5973	757					
C_4F_{10}	**PoraBOND**	**5975**	**599**	119	219	131	0.0042	0.0180
	GasPro	**5973**	**794**	119	219	150	0.0067	0.0249
$CBrClF_2$ [H-1211]	PoraBOND	5975	669					
	GasPro	5973	823					
CH_3CCl_2F [HCFC-142b]	PoraBOND	5975	678					
	GasPro	5973	856					
C_5F_{12}	**PoraBOND**	**5975**	**676**	119	169	–	0.0021	0.0120
	GasPro	**5973**	**873**	119	169	181	0.0029	0.0096
$C_3H_2F_6$ [HFC-236fa]	PoraBOND	5975	617					
	GasPro	5973	876					
CH_2Cl_2	PoraBOND	5975	717					
	GasPro	5973	939					
C_6F_{14}	**PoraBOND**	**5975**	**742**	169	119	–	0.0040	0.0057
	GasPro	**5973**	**948**	119	169	219	0.0065	0.0117
$C_2H_3Cl_2F$ [HCFC-141b]	PoraBOND	5975	741					
	GasPro	5973	965					
CCl_4	PoraBOND	5975	849					
	GasPro	5973	1035					
C_7F_{16}	**PoraBOND**	**5975**	**800**	219	169	–	0.0042	0.0048
	GasPro	**5973**	**1040**	169	219	–	0.0021	0.0129
$C_4H_5F_5$ [HFC-365mfc]	PoraBOND	5975	672					
	GasPro	5973	1067					
CH_3CCl_3	PoraBOND	5975	841					
	GasPro	5973	1124					
C_8F_{18}	**PoraBOND**	**5975**	**855**	219	269	–	0.0026	0.0102
	GasPro	**5973**	**1168**	219	119	69	0.0032	0.0153
C_2Cl_4 [PCE]	PoraBOND	5975	959					
	GasPro	5973	1194					

* Additional compounds are shown for reference. Parameters for the oven are: ramping from 40° C to 200° C over 7 minutes for both the GasPro and PoraBOND with the ovens subsequently held at 200° C. The pressure is ramping at the same time to maintain a constant flow from 6.1 to 15.1 psig for the PoraBOND column and from 9 to 18 psig for the GasPro and subsequently held constant. Standard precisions refer to the 1-σ standard deviation taken on the working standard used, which is a NH 2010 sample for the SIO Medusa and a 2010 sample filled at Cape Grim for the CSIRO Medusa. Species in bold are those discussed in this study. Non-bolded species are added for reference.

blank was detected for C_6F_{14}, C_7F_{16} and C_8F_{18} (0.008 and 0.005 ppt for C_6F_{14}, 0.012 and 0.013 ppt for C_7F_{16}, 0.017 and 0.016 ppt for C_8F_{18} on the CSIRO and SIO instruments, respectively), most likely due to the Nafion dryers used in the Medusa, and the observations were corrected accordingly. The detection limits for each species on both instruments were estimated as three times the baseline height of the noise of the target ion immediately preceding and following the elution of the species and are presented in Table 2. The differences in the detection limits between the two instruments are due to the improved separation of analytes on the GS-GasPro column used on the CSIRO Medusa and the newer model of MS (5975) used at SIO.

Two experiments were done to assess whether the instrument responses of the Medusa systems were linear over the required range of mixing ratios for each species. In general, the instrument response, R, is related to the sample mole fractions, χ, by $R \propto \chi^{(1-\epsilon)}$, where ϵ is the nonlinearity parameter (Prinn et al., 2000). A whole-air sample from a 2010 Cape Grim Air Archive (CGAA) tank was decanted into a 35-l stainless steel tank (Essex Cryogenics), and spiked with a small volume of high-purity methane (CH_4) to increase the CH_4 mole fractions from ambient to ca. 8 parts per million. From this spiked air sample, six subsamples were prepared in 6-l stainless steel SilcoCan flasks (Restek Inc.) using a vacuum manifold. Each subsample was then diluted by

adding "zero-air". The zero-air was measured on the Medusa and found to be analyte free for the PFCs studied here. The amount of zero-air added was varied to give a range of dilution factors (nominally from 6.25 % to 75 %). The actual dilution factors for each subsample were determined by precisely measuring the CH_4 mole fraction (including that of the spiked parent sample) on a gas chromatography-flame ionization detector (GC-FID) system with a known linear response (Francey et al., 2003). These subsamples were subsequently measured on the Medusa systems to determine the linearity of the Medusa measurements for each species. All but the lowest concentration subsample of 6.25 % were above the detection limit for C_4F_{10}, C_5F_{12}, C_7F_{16} and C_8F_{18}. The lowest concentration subsample was slightly above the detection limit for C_6F_{14}.

The second experiment to characterize the instrument response involved sampling different volumes from a single air sample (Miller et al., 2008). The range of relative volumes sampled was from 6 % to 200 % of the standard 2-l sample. The volume method has the advantage of characterizing instrument responses at mole fractions above present day background levels, which could not be easily achieved through the dilution subsamples unless more concentrated samples were prepared. However, as the atmospheric samples measured in the air archives were all below current atmospheric background mole fractions, the volume method served only to complement the dilution method's instrument response experiment. Generally, the systems exhibited a linear response over much of the required range of mole fractions, with departures from linearity at mole fractions corresponding to those of the oldest archive samples, which have the lowest mole fractions. Based on these dilution experiment measurements, a nonlinearity parameter, ϵ, was estimated for each PFC on each instrument and was used to correct the observations. These nonlinearity parameters were relatively small and ranged from 0 to 0.047, with the largest nonlinearity correction required for C_8F_{18}.

2.2 Calibration

Four primary standards were prepared at SIO to identify and quantify the heavy PFCs on the Medusa. The primary standards were prepared following the bootstrap method by stepwise dilution, with dichlorodifluoromethane (CCl_2F_2, CFC-12) used as the bootstrap gas (Prinn et al., 2000). The high-purity compounds were purchased from Synquest Laboratories with purities of: C_4F_{10} (98 % min.), C_5F_{12} (99 % min.), C_6F_{14} (98.5 % min.), C_7F_{16} (98 % min.) and C_8F_{18} (99 % min.); the nitrous oxide (N_2O) was purchased from Scott Specialty Gases and had a purity of 99.9997 %, and CFC-12 had a purity of 99.99 %. Each high-purity compound was vacuum distilled for further purification by repeated cycles of freezing with liquid nitrogen, vacuum removal of noncondensable contaminants and then thawing.

First a gravimetric PFC/CFC-12/N_2O mixture was prepared with a molar ratio of PFC to CFC-12 of 1.85–3.7×10^{-3}, with CFC-12 being used as the bootstrap gas and N_2O as the balance gas. Typically N_2O is used as the bootstrap gas; however these standards were prepared as standard additions and the expected final N_2O mole fractions would have been beyond the range of the currently available SIO calibration scale. Therefore, CFC-12 was used as the bootstrap gas, as the resulting final mole fractions of CFC-12 can be accurately measured on the Medusa.

A primary standard was prepared by spiking a real air sample filled at La Jolla, CA (32.87° N, 117.25° W) with the PFC/CFC-12/N_2O mixture. The real air sample was measured on the SIO Medusa to measure its initial CFC-12 mole fraction and instrument response for each PFC. The additional mole fractions added to the real air sample from the PFC/CFC-12/N_2O spike were ca. 2 parts per trillion (ppt) of C_6F_{14}, 1 ppt of the other PFCs and 540 ppt of CFC-12. The enhancement factor of the PFC/CFC-12/N_2O mixture added to the real air sample was determined by measuring the final CFC-12 mole fractions on the Medusa. The final atmospheric mole fractions in the primary standard were estimated as described by Ellison and Thompson (2008).

The primary standards were measured on the Medusa to determine the retention times and mass spectra of the heavy PFCs as well as to quantify the atmospheric observations. The mass spectra of the high molecular weight PFCs agree with published spectra from the National Institute of Standards and Technology and the retention times are consistent with what is expected based on their boiling points (NIST, 2011). Table 2 shows the target and qualifier mass-to-charge ratios, as well as the retention times, used on the SIO and CSIRO Medusa systems; the target mass-to-charge ratio is used for identification and quantitation, while the qualifiers are only used for ensuring the proper identification of the species. Four primary standards were prepared and the calibration scale, referred to as SIO-2012, has estimated accuracies of 6.8 % for C_4F_{10}, 7.8 % for C_5F_{12}, 4.0 % for C_6F_{14}, 6.6 % for C_7F_{16} and 7.9 % for C_8F_{18}.

3 Archived air samples

The atmospheric histories of these heavy PFCs are based on measurements made at SIO and CSIRO of NH and SH archived air samples, which cover a 39-year period. In total, 36 NH separate samples (33 measured at SIO and 3 measured at CSIRO) with fill dates from 1973 to 2011 were measured. These tanks were filled either at Cape Meares, Oregon (45.50° N, 123.95° W), La Jolla, California (32.87° N, 117.25° W) or Trinidad Head, California (41.05° N, 124.05° W) and one tank at Harvard Forest, Massachusetts (42.53° N, 72.19° W) during baseline conditions and are from the laboratories of R.F. Weiss; R.F. Keeling; and the late C.D. Keeling at SIO. The fill techniques, tank

Table 3. Northern and Southern Hemisphere and Global Average Annual Mean Mole Fractions and Growth Rates and Associated Uncertainties 1980-2011 for C_4F_{10}.*

Year	Northern Hemisphere		Southern Hemisphere		Global Average	
	Mole Fraction [ppt]	Growth Rate [ppq yr^{-1}]	Mole Fraction [ppt]	Growth Rate [ppq yr^{-1}]	Mole Fraction [ppt]	Growth Rate [ppq yr^{-1}]
1980	0.021 ± 0.009	3.3 ± 1.5	0.019 ± 0.015	3.6 ± 4.0	0.020 ± 0.012	3.5 ± 2.8
1981	0.025 ± 0.009	4.4 ± 1.5	0.023 ± 0.013	3.7 ± 3.0	0.024 ± 0.011	4.0 ± 2.3
1982	0.030 ± 0.007	5.2 ± 1.5	0.026 ± 0.012	3.8 ± 2.3	0.028 ± 0.010	4.5 ± 1.9
1983	0.035 ± 0.006	5.7 ± 1.4	0.030 ± 0.011	4.0 ± 1.9	0.033 ± 0.009	4.9 ± 1.7
1984	0.041 ± 0.005	6.1 ± 1.2	0.034 ± 0.010	4.1 ± 1.8	0.038 ± 0.007	5.1 ± 1.5
1985	0.047 ± 0.004	6.3 ± 1.0	0.039 ± 0.008	4.3 ± 1.7	0.043 ± 0.006	5.3 ± 1.4
1986	0.054 ± 0.003	6.4 ± 0.9	0.043 ± 0.007	4.6 ± 1.6	0.048 ± 0.005	5.5 ± 1.3
1987	0.060 ± 0.003	6.4 ± 0.7	0.048 ± 0.006	4.8 ± 1.5	0.054 ± 0.004	5.6 ± 1.1
1988	0.067 ± 0.002	6.3 ± 0.6	0.053 ± 0.004	5.1 ± 1.3	0.060 ± 0.003	5.7 ± 1.0
1989	0.073 ± 0.002	6.1 ± 0.5	0.058 ± 0.003	5.4 ± 1.1	0.065 ± 0.003	5.7 ± 0.8
1990	0.079 ± 0.002	5.9 ± 0.5	0.063 ± 0.003	5.7 ± 0.9	0.071 ± 0.002	5.8 ± 0.7
1991	0.085 ± 0.002	5.7 ± 0.4	0.069 ± 0.002	5.8 ± 0.7	0.077 ± 0.002	5.8 ± 0.5
1992	0.090 ± 0.002	5.6 ± 0.4	0.075 ± 0.002	6.0 ± 0.5	0.083 ± 0.002	5.8 ± 0.5
1993	0.096 ± 0.002	5.6 ± 0.5	0.081 ± 0.002	6.1 ± 0.5	0.088 ± 0.002	5.8 ± 0.5
1994	0.101 ± 0.003	5.5 ± 0.5	0.087 ± 0.002	6.2 ± 0.4	0.094 ± 0.002	5.8 ± 0.5
1995	0.107 ± 0.003	5.5 ± 0.6	0.093 ± 0.002	6.2 ± 0.4	0.100 ± 0.002	5.9 ± 0.5
1996	0.112 ± 0.003	5.6 ± 0.7	0.100 ± 0.002	6.3 ± 0.4	0.106 ± 0.002	5.9 ± 0.6
1997	0.118 ± 0.003	5.7 ± 0.8	0.106 ± 0.002	6.3 ± 0.5	0.112 ± 0.003	6.0 ± 0.7
1998	0.124 ± 0.004	5.8 ± 1.1	0.112 ± 0.002	6.4 ± 0.6	0.118 ± 0.003	6.1 ± 0.8
1999	0.130 ± 0.004	5.8 ± 1.3	0.119 ± 0.002	6.5 ± 0.6	0.124 ± 0.003	6.2 ± 1.0
2000	0.135 ± 0.005	5.8 ± 1.5	0.125 ± 0.002	6.4 ± 0.6	0.130 ± 0.004	6.1 ± 1.1
2001	0.141 ± 0.006	5.6 ± 1.8	0.132 ± 0.003	6.1 ± 0.5	0.136 ± 0.004	5.9 ± 1.2
2002	0.147 ± 0.007	5.2 ± 1.8	0.138 ± 0.003	5.7 ± 0.6	0.142 ± 0.005	5.5 ± 1.2
2003	0.152 ± 0.008	4.8 ± 1.4	0.143 ± 0.002	5.1 ± 0.7	0.147 ± 0.005	5.0 ± 1.0
2004	0.156 ± 0.009	4.3 ± 0.9	0.148 ± 0.002	4.4 ± 0.7	0.152 ± 0.006	4.3 ± 0.8
2005	0.160 ± 0.009	3.7 ± 1.3	0.152 ± 0.002	3.7 ± 0.6	0.156 ± 0.006	3.7 ± 1.0
2006	0.164 ± 0.008	3.2 ± 1.8	0.155 ± 0.002	3.2 ± 0.6	0.159 ± 0.005	3.2 ± 1.2
2007	0.167 ± 0.007	2.8 ± 2.0	0.158 ± 0.002	2.7 ± 0.6	0.162 ± 0.004	2.7 ± 1.3
2008	0.169 ± 0.006	2.6 ± 1.9	0.161 ± 0.002	2.4 ± 0.6	0.165 ± 0.004	2.5 ± 1.2
2009	0.172 ± 0.006	2.4 ± 1.6	0.163 ± 0.002	2.3 ± 0.7	0.167 ± 0.004	2.3 ± 1.1
2010	0.174 ± 0.005	2.2 ± 1.5	0.165 ± 0.002	2.3 ± 0.9	0.170 ± 0.004	2.3 ± 1.2
2011	0.176 ± 0.005	2.0 ± 1.8	0.168 ± 0.002	2.4 ± 1.0	0.172 ± 0.004	2.2 ± 1.4

* Annual hemispheric mean mole fractions and growth rates are estimated from the smoothing cubic spline fits.

materials, tank sizes and fill purposes of these samples varied. Two tanks were identified as outliers with atmospheric mole fractions significantly higher than present day values. One 1978 tank was rejected for C_4F_{10} and C_5F_{12}, but a second tank with an identical fill date was also measured. Additionally a 1974 tank was rejected for C_8F_{18}, as samples with similar fill dates were below the detection limit. From 2003 onward, a collection of tanks containing NH air have been maintained at R.F. Weiss's laboratory at SIO as an air archive. These samples were pumped into 35-l internally electropolished stainless steel cylinders (Essex Cryogenics) at Trinidad Head, California using a modified oil-free compressor (Rix Industries). Recent filled archive tanks agree with in situ measurements made by the Medusa system at the time of the tank filling for the high molecular weight PFCs studied here,

confirming that the modified Rix compressor does not compromise the integrity of these samples for the high molecular weight PFCs.

Forty-six separate SH samples filled between 1978 and 2010 were also measured (6 at SIO and 40 at CSIRO). All but three of these samples, which were from the M.A. Wahlen laboratory at SIO, are part of the CGAA collection (Krummel et al., 2007; Langenfelds et al., 1996). The CGAA samples analyzed as part of this study consist of whole-air samples cryogenically filled in 35-l internally electropolished stainless steel cylinders at the Cape Grim Baseline Air Pollution Station in Tasmania, Australia (40.68° S, 144.69° E), except for three which were cryogenically collected in 48-l aluminum cylinders; these latter three samples were rejected for C_8F_{18}, as their values were significantly higher

Table 4. Northern and Southern Hemisphere and Global Average Annual Mean Mole Fractions and Growth Rates and Associated Uncertainties 1980-2011 for C_5F_{12}.*

Year	Northern Hemisphere		Southern Hemisphere		Global Average	
	Mole Fraction [ppt]	Growth Rate [ppq yr^{-1}]	Mole Fraction [ppt]	Growth Rate [ppq yr^{-1}]	Mole Fraction [ppt]	Growth Rate [ppq yr^{-1}]
1980	0.018 ± 0.002	2.2 ± 0.7	0.012 ± 0.001	2.7 ± 0.2	0.015 ± 0.001	2.4 ± 0.4
1981	0.020 ± 0.001	2.5 ± 0.5	0.015 ± 0.001	2.7 ± 0.2	0.018 ± 0.001	2.6 ± 0.4
1982	0.023 ± 0.001	3.0 ± 0.4	0.018 ± 0.001	2.8 ± 0.2	0.020 ± 0.001	2.9 ± 0.3
1983	0.026 ± 0.001	3.5 ± 0.3	0.021 ± 0.001	2.8 ± 0.1	0.023 ± 0.001	3.2 ± 0.2
1984	0.030 ± 0.001	4.0 ± 0.3	0.024 ± 0.001	3.0 ± 0.1	0.027 ± 0.001	3.5 ± 0.2
1985	0.034 ± 0.001	4.4 ± 0.3	0.027 ± 0.001	3.1 ± 0.1	0.030 ± 0.001	3.8 ± 0.2
1986	0.039 ± 0.001	4.7 ± 0.4	0.030 ± 0.001	3.3 ± 0.2	0.034 ± 0.001	4.0 ± 0.3
1987	0.043 ± 0.002	4.9 ± 0.5	0.033 ± 0.001	3.5 ± 0.2	0.038 ± 0.001	4.2 ± 0.4
1988	0.048 ± 0.002	4.9 ± 0.7	0.037 ± 0.001	3.7 ± 0.2	0.043 ± 0.001	4.3 ± 0.4
1989	0.053 ± 0.002	4.9 ± 0.8	0.041 ± 0.001	4.0 ± 0.2	0.047 ± 0.002	4.5 ± 0.5
1990	0.058 ± 0.003	4.9 ± 0.9	0.045 ± 0.001	4.3 ± 0.2	0.051 ± 0.002	4.6 ± 0.6
1991	0.063 ± 0.004	4.9 ± 1.0	0.049 ± 0.001	4.6 ± 0.3	0.056 ± 0.003	4.7 ± 0.6
1992	0.068 ± 0.005	4.8 ± 1.1	0.054 ± 0.001	4.9 ± 0.3	0.061 ± 0.003	4.8 ± 0.7
1993	0.073 ± 0.006	4.8 ± 1.1	0.059 ± 0.001	5.1 ± 0.3	0.066 ± 0.004	4.9 ± 0.7
1994	0.077 ± 0.007	4.7 ± 1.1	0.064 ± 0.002	5.2 ± 0.3	0.071 ± 0.004	5.0 ± 0.7
1995	0.082 ± 0.008	4.6 ± 1.0	0.069 ± 0.002	5.3 ± 0.3	0.076 ± 0.005	5.0 ± 0.6
1996	0.087 ± 0.009	4.5 ± 0.9	0.075 ± 0.002	5.3 ± 0.2	0.081 ± 0.005	4.9 ± 0.5
1997	0.091 ± 0.010	4.3 ± 0.7	0.080 ± 0.002	5.2 ± 0.2	0.085 ± 0.006	4.8 ± 0.5
1998	0.095 ± 0.010	4.1 ± 0.6	0.085 ± 0.002	5.0 ± 0.3	0.090 ± 0.006	4.6 ± 0.5
1999	0.099 ± 0.011	3.9 ± 0.8	0.090 ± 0.002	4.8 ± 0.3	0.095 ± 0.006	4.3 ± 0.6
2000	0.103 ± 0.010	3.6 ± 1.3	0.094 ± 0.001	4.5 ± 0.3	0.099 ± 0.006	4.0 ± 0.8
2001	0.107 ± 0.010	3.2 ± 1.9	0.099 ± 0.001	4.1 ± 0.3	0.103 ± 0.005	3.6 ± 1.1
2002	0.110 ± 0.009	2.8 ± 2.1	0.103 ± 0.001	3.7 ± 0.3	0.106 ± 0.005	3.2 ± 1.2
2003	0.112 ± 0.008	2.5 ± 2.1	0.106 ± 0.001	3.1 ± 0.3	0.109 ± 0.004	2.8 ± 1.2
2004	0.115 ± 0.007	2.2 ± 1.9	0.109 ± 0.001	2.6 ± 0.2	0.112 ± 0.004	2.4 ± 1.1
2005	0.117 ± 0.006	2.0 ± 1.8	0.111 ± 0.001	2.2 ± 0.3	0.114 ± 0.004	2.1 ± 1.0
2006	0.119 ± 0.006	1.8 ± 1.8	0.113 ± 0.001	1.8 ± 0.3	0.116 ± 0.004	1.8 ± 1.0
2007	0.120 ± 0.006	1.6 ± 1.7	0.115 ± 0.001	1.6 ± 0.3	0.118 ± 0.004	1.6 ± 1.0
2008	0.122 ± 0.007	1.4 ± 1.5	0.117 ± 0.001	1.4 ± 0.3	0.119 ± 0.004	1.4 ± 0.9
2009	0.123 ± 0.007	1.3 ± 1.2	0.118 ± 0.001	1.4 ± 0.4	0.121 ± 0.004	1.4 ± 0.8
2010	0.124 ± 0.008	1.3 ± 1.3	0.119 ± 0.001	1.4 ± 0.5	0.122 ± 0.004	1.3 ± 0.9
2011	0.126 ± 0.007	1.3 ± 2.1	0.121 ± 0.002	1.4 ± 0.6	0.123 ± 0.004	1.4 ± 1.4

* Annual hemispheric mean mole fractions and growth rates are estimated from the smoothing cubic spline fits.

than present-day background mole fractions. Five archive samples, all collected in 2001 and 2002, had significantly higher than current baseline mole fractions for C_7F_{16} and these values were consequently flagged as contaminated; these included the three samples from the M. A. Wahlen laboratory and two CGAA samples. These five samples were all stored in stainless steel cylinders, therefore most likely a local source at the Cape Grim Station influenced these samples. The Wahlen samples were also rejected for C_6F_{14}, as an unidentified analyte coeluted with C_6F_{14}.

Seven subsamples of the CGAA, covering the time period of 1986 to 2008, were decanted into 4.5-l internally electropolished stainless steel cylinders (Essex Cryogenics) and subsequently measured on the SIO Medusa system; the parent samples were measured at CSIRO. This was to verify whether the two instruments and the calibration propagations produced measurements that agreed within known uncertainties. Generally, the measurements on the two systems agreed well within the measurement uncertainty. The most notable difference between the two instruments was for C_8F_{18}, with a maximum difference of 0.009 ppt, which was 12 % of the sample concentration.

For both sets of archived samples, at least 3 replicate measurements were made of each sample; for younger samples, 5 to 6 replicate measurements were made since more air was available. The measurement errors on the samples are estimated as the 1-σ standard deviations of the repeat measurements, and samples below the detection limit of the Medusa were assigned a measurement error equal to that of the detection limit for the purpose of data fitting. The archived air

Table 5. Northern and Southern Hemisphere and Global Average Annual Mean Mole Fractions and Growth Rates and Associated Uncertainties 1980-2011 for C_6F_{14}.[*]

Year	Northern Hemisphere		Southern Hemisphere		Global Average	
	Mole Fraction [ppt]	Growth Rate [ppq yr^{-1}]	Mole Fraction [ppt]	Growth Rate [ppq yr^{-1}]	Mole Fraction [ppt]	Growth Rate [ppq yr^{-1}]
1980	0.003 ± 0.002	0.0 ± 0.6	0.008 ± 0.008	2.7 ± 1.3	0.005 ± 0.005	1.4 ± 0.9
1981	0.003 ± 0.002	0.0 ± 0.6	0.010 ± 0.007	2.9 ± 1.2	0.007 ± 0.004	1.5 ± 0.9
1982	0.003 ± 0.002	-0.3 ± 0.6	0.013 ± 0.006	3.1 ± 1.1	0.008 ± 0.004	1.4 ± 0.9
1983	0.002 ± 0.002	-0.2 ± 0.6	0.017 ± 0.005	3.3 ± 1.0	0.010 ± 0.004	1.6 ± 0.8
1984	0.003 ± 0.003	1.3 ± 0.4	0.020 ± 0.004	3.5 ± 0.9	0.011 ± 0.003	2.4 ± 0.7
1985	0.005 ± 0.003	3.2 ± 0.3	0.024 ± 0.003	3.6 ± 0.8	0.014 ± 0.003	3.4 ± 0.6
1986	0.009 ± 0.003	5.0 ± 0.3	0.027 ± 0.002	3.6 ± 0.7	0.018 ± 0.003	4.3 ± 0.5
1987	0.015 ± 0.003	6.8 ± 0.4	0.031 ± 0.002	3.7 ± 0.6	0.023 ± 0.002	5.3 ± 0.5
1988	0.022 ± 0.002	8.4 ± 0.5	0.035 ± 0.002	3.9 ± 0.5	0.029 ± 0.002	6.2 ± 0.5
1989	0.032 ± 0.002	10.0 ± 0.6	0.039 ± 0.001	4.1 ± 0.4	0.035 ± 0.002	7.0 ± 0.5
1990	0.042 ± 0.002	11.3 ± 0.7	0.043 ± 0.001	4.6 ± 0.3	0.043 ± 0.002	8.0 ± 0.5
1991	0.054 ± 0.003	12.4 ± 0.8	0.048 ± 0.001	5.4 ± 0.3	0.051 ± 0.002	8.9 ± 0.6
1992	0.067 ± 0.003	13.4 ± 1.0	0.054 ± 0.001	6.4 ± 0.3	0.060 ± 0.002	9.9 ± 0.6
1993	0.081 ± 0.004	14.2 ± 1.2	0.061 ± 0.001	7.7 ± 0.3	0.071 ± 0.003	11.0 ± 0.7
1994	0.095 ± 0.005	14.9 ± 1.3	0.069 ± 0.001	9.4 ± 0.3	0.082 ± 0.003	12.1 ± 0.8
1995	0.110 ± 0.006	15.4 ± 1.3	0.079 ± 0.001	11.3 ± 0.3	0.095 ± 0.004	13.3 ± 0.8
1996	0.126 ± 0.007	15.8 ± 1.3	0.092 ± 0.002	13.3 ± 0.4	0.109 ± 0.004	14.5 ± 0.8
1997	0.142 ± 0.009	16.0 ± 1.2	0.106 ± 0.002	15.2 ± 0.4	0.124 ± 0.005	15.6 ± 0.8
1998	0.158 ± 0.010	16.1 ± 1.0	0.122 ± 0.002	16.7 ± 0.5	0.140 ± 0.006	16.4 ± 0.7
1999	0.174 ± 0.011	15.6 ± 0.6	0.139 ± 0.002	17.6 ± 0.5	0.156 ± 0.006	16.6 ± 0.5
2000	0.189 ± 0.011	14.5 ± 0.7	0.156 ± 0.002	17.5 ± 0.5	0.173 ± 0.007	16.0 ± 0.6
2001	0.203 ± 0.010	12.6 ± 1.4	0.174 ± 0.002	16.5 ± 0.4	0.188 ± 0.006	14.6 ± 0.9
2002	0.214 ± 0.009	10.8 ± 1.9	0.189 ± 0.003	14.9 ± 0.5	0.202 ± 0.006	12.8 ± 1.2
2003	0.224 ± 0.008	9.3 ± 2.0	0.203 ± 0.002	12.9 ± 0.6	0.214 ± 0.005	11.1 ± 1.3
2004	0.233 ± 0.006	8.1 ± 1.8	0.215 ± 0.002	11.0 ± 0.7	0.224 ± 0.004	9.5 ± 1.2
2005	0.241 ± 0.005	7.2 ± 1.5	0.226 ± 0.002	9.3 ± 0.7	0.233 ± 0.003	8.3 ± 1.1
2006	0.248 ± 0.004	6.4 ± 1.3	0.234 ± 0.002	8.0 ± 0.6	0.241 ± 0.003	7.2 ± 1.0
2007	0.254 ± 0.003	5.5 ± 1.2	0.242 ± 0.002	6.9 ± 0.6	0.248 ± 0.003	6.2 ± 0.9
2008	0.259 ± 0.003	4.4 ± 1.1	0.248 ± 0.002	6.0 ± 0.7	0.253 ± 0.003	5.2 ± 0.9
2009	0.263 ± 0.003	3.7 ± 1.1	0.254 ± 0.002	5.5 ± 0.7	0.258 ± 0.003	4.6 ± 0.9
2010	0.266 ± 0.004	3.7 ± 1.1	0.259 ± 0.002	5.3 ± 0.7	0.263 ± 0.003	4.5 ± 0.9
2011	0.270 ± 0.005	4.9 ± 1.0	0.264 ± 0.002	5.1 ± 0.7	0.267 ± 0.003	5.0 ± 0.9

[*]Annual hemispheric mean mole fractions and growth rates are estimated from the smoothing cubic spline fits.

sample measurements for both sets of archives are provided in the supplementary material.

4 Results and discussion

The atmospheric histories from 1973 to 2011 for the high molecular weight PFCs studied here are shown in Figs. 1–5. Due to the sparseness of the available data set, the presented annual mean mole fractions and growth rates are based on cubic smoothed spline fits to the observations. The observations were weighted by their measurement uncertainty and a 50 % attenuation period of 4 years was used, which is slightly larger than the mean data-spacing, in estimating the smoothing splines (Enting et al., 2006). The uncertainties associated with the spline fits were estimated using a Monte Carlo approach, where the fitting was repeated 1000 times with randomly varied observations that had distributions based on their measurement uncertainty. The uncertainty on each spline fit was taken as the 1-σ standard deviation of these runs. The growth rate was also calculated for each of the 1000 runs and the uncertainty associated with the annual growth rate was estimated as the 1-σ standard deviation of the calculated growth rates. The smoothed spline fits are shown along with the observations in Figs. 1–5. The bottom panels of Figs. 1–5 show the annual hemispheric growth rates estimated from the cubic smoothed spline fits for each PFC. The annual mean mole fractions and growth rates from the spline fits are presented in Tables 3–7.

C_4F_{10} and C_5F_{12} are present in the earliest archived samples at 0.015 ppt and 0.011 ppt respectively, but these

Table 6. Northern and Southern Hemisphere and Global Average Annual Mean Mole Fractions and Growth Rates and Associated Uncertainties 1980-2011 for C_7F_{16}.[*]

Year	Northern Hemisphere		Southern Hemisphere		Global Average	
	Mole Fraction [ppt]	Growth Rate [ppq yr^{-1}]	Mole Fraction [ppt]	Growth Rate [ppq yr^{-1}]	Mole Fraction [ppt]	Growth Rate [ppq yr^{-1}]
1980	0.000 ± 0.002	0.3 ± 0.5	0.011 ± 0.008	1.9 ± 1.6	0.005 ± 0.005	1.1 ± 1.0
1981	0.000 ± 0.002	0.6 ± 0.5	0.013 ± 0.007	1.9 ± 1.3	0.006 ± 0.004	1.2 ± 0.9
1982	0.001 ± 0.002	1.0 ± 0.5	0.015 ± 0.006	2.0 ± 1.1	0.008 ± 0.004	1.5 ± 0.8
1983	0.002 ± 0.002	1.7 ± 0.5	0.017 ± 0.005	2.1 ± 0.9	0.009 ± 0.004	1.9 ± 0.7
1984	0.004 ± 0.002	2.5 ± 0.4	0.019 ± 0.005	2.2 ± 0.8	0.011 ± 0.004	2.3 ± 0.6
1985	0.007 ± 0.003	3.3 ± 0.3	0.021 ± 0.004	2.3 ± 0.8	0.014 ± 0.003	2.8 ± 0.6
1986	0.011 ± 0.003	4.0 ± 0.4	0.023 ± 0.003	2.5 ± 0.7	0.017 ± 0.003	3.3 ± 0.5
1987	0.015 ± 0.003	4.6 ± 0.4	0.026 ± 0.003	2.7 ± 0.6	0.020 ± 0.003	3.7 ± 0.5
1988	0.020 ± 0.003	5.0 ± 0.5	0.029 ± 0.002	3.0 ± 0.6	0.024 ± 0.002	4.0 ± 0.5
1989	0.025 ± 0.003	5.4 ± 0.6	0.032 ± 0.002	3.2 ± 0.5	0.028 ± 0.002	4.3 ± 0.5
1990	0.030 ± 0.003	5.6 ± 0.7	0.035 ± 0.001	3.5 ± 0.4	0.033 ± 0.002	4.5 ± 0.6
1991	0.036 ± 0.003	5.6 ± 0.8	0.039 ± 0.001	3.7 ± 0.3	0.037 ± 0.002	4.6 ± 0.6
1992	0.042 ± 0.004	5.5 ± 1.0	0.043 ± 0.001	3.9 ± 0.3	0.042 ± 0.002	4.7 ± 0.6
1993	0.047 ± 0.004	5.3 ± 1.2	0.046 ± 0.001	4.0 ± 0.2	0.047 ± 0.003	4.6 ± 0.7
1994	0.052 ± 0.005	5.1 ± 1.2	0.051 ± 0.001	4.1 ± 0.2	0.051 ± 0.003	4.6 ± 0.7
1995	0.057 ± 0.006	4.9 ± 1.2	0.055 ± 0.001	4.1 ± 0.3	0.056 ± 0.004	4.5 ± 0.7
1996	0.062 ± 0.007	4.7 ± 1.1	0.059 ± 0.001	4.1 ± 0.3	0.060 ± 0.004	4.4 ± 0.7
1997	0.067 ± 0.008	4.5 ± 0.9	0.063 ± 0.001	4.1 ± 0.3	0.065 ± 0.005	4.3 ± 0.6
1998	0.071 ± 0.009	4.4 ± 0.6	0.067 ± 0.001	4.0 ± 0.3	0.069 ± 0.005	4.2 ± 0.5
1999	0.075 ± 0.009	4.3 ± 0.3	0.071 ± 0.002	4.0 ± 0.3	0.073 ± 0.006	4.1 ± 0.3
2000	0.080 ± 0.010	4.2 ± 0.6	0.075 ± 0.002	3.8 ± 0.2	0.077 ± 0.006	4.0 ± 0.4
2001	0.084 ± 0.009	4.1 ± 1.1	0.079 ± 0.002	3.7 ± 0.1	0.081 ± 0.006	3.9 ± 0.6
2002	0.088 ± 0.008	4.1 ± 1.4	0.082 ± 0.002	3.5 ± 0.2	0.085 ± 0.005	3.8 ± 0.8
2003	0.092 ± 0.007	4.0 ± 1.6	0.086 ± 0.002	3.4 ± 0.3	0.089 ± 0.004	3.7 ± 0.9
2004	0.096 ± 0.005	3.9 ± 1.6	0.089 ± 0.002	3.3 ± 0.4	0.092 ± 0.004	3.6 ± 1.0
2005	0.100 ± 0.004	3.8 ± 1.5	0.092 ± 0.001	3.3 ± 0.4	0.096 ± 0.003	3.6 ± 0.9
2006	0.103 ± 0.004	3.7 ± 1.4	0.096 ± 0.001	3.4 ± 0.3	0.100 ± 0.002	3.5 ± 0.8
2007	0.107 ± 0.004	3.7 ± 1.3	0.099 ± 0.001	3.5 ± 0.3	0.103 ± 0.002	3.6 ± 0.8
2008	0.111 ± 0.005	3.6 ± 1.1	0.103 ± 0.001	3.6 ± 0.3	0.107 ± 0.003	3.6 ± 0.7
2009	0.114 ± 0.005	3.4 ± 1.0	0.106 ± 0.001	3.7 ± 0.3	0.110 ± 0.003	3.6 ± 0.6
2010	0.118 ± 0.006	3.2 ± 1.1	0.110 ± 0.001	3.7 ± 0.3	0.114 ± 0.003	3.5 ± 0.7
2011	0.121 ± 0.006	3.0 ± 1.6	0.114 ± 0.001	3.7 ± 0.3	0.117 ± 0.004	3.4 ± 1.0

[*] Annual hemispheric mean mole fractions and growth rates are estimated from the smoothing cubic spline fits.

measurements are considered below the estimated detection limits of the instruments, see Fig. 1 and Fig. 2. Analysis of firn air samples from Greenland confirm that there is no detectable natural abundance for these PFCs. C_4F_{10} and C_5F_{12} exhibit quasi-exponential growth in the 1980s and then grow nearly linearly to present day globally averaged (taken as the average between the NH and SH spline fit data) background atmospheric mole fractions of 0.17 ppt and 0.12 ppt, respectively. The slowdown in growth rates in the the 2000s suggest that emissions are decreasing, as is supported by the decline in the inter-hemispheric gradients seen in the observations, for C_4F_{10} and C_5F_{12}. Emissions of these high molecular weight PFCs based on EDGARv4.2 are of anthropogenic origin and primarily released in the NH (ER-JRC/PBL, 2009). Therefore as is expected, we see higher atmospheric mole

fractions in the NH than in the SH due to the 1 to 2 year mixing time between the two hemispheres. This is confirmed by the lag in the SH growth rate as compared to that estimated in the NH. Higher variability in the NH samples can be seen in the early years for C_4F_{10} and C_5F_{12}, as compared to the SH samples. This is attributed to sampling of less well mixed air due to emissions originating primarily in the NH, although efforts were made to fill the archive tanks during baseline conditions.

C_6F_{14} and C_7F_{16} are not detectable in the archived samples until 1984-1985 and grow quasi-exponentially until 1999 and 1992, respectively, see Fig. 3 and Fig. 4. C_8F_{18} follows a similar trend to that of C_6F_{14}, although it is not detectable until the mid 1990s, see Fig. 5, which is most likely due to lower emission rates. C_6F_{14} is the most abundant of

Table 7. Northern and Southern Hemisphere and Global Average Annual Mean Mole Fractions and Growth Rates and Associated Uncertainties 1980–2011 for C_8F_{18}.*

	Northern Hemisphere		Southern Hemisphere		Global Average	
Year	Mole Fraction [ppt]	Growth Rate [ppq yr^{-1}]	Mole Fraction [ppt]	Growth Rate [ppq yr^{-1}]	Mole Fraction [ppt]	Growth Rate [ppq yr^{-1}]
1980	0.001 ± 0.004	0.4 ± 1.3	0.011 ± 0.009	0.5 ± 2.9	0.006 ± 0.006	0.5 ± 2.1
1981	0.001 ± 0.004	0.4 ± 1.4	0.012 ± 0.007	0.4 ± 2.7	0.007 ± 0.006	0.4 ± 2.1
1982	0.002 ± 0.004	0.3 ± 1.5	0.012 ± 0.007	0.4 ± 2.4	0.007 ± 0.006	0.3 ± 1.9
1983	0.002 ± 0.004	0.3 ± 1.5	0.012 ± 0.007	0.4 ± 2.0	0.007 ± 0.006	0.3 ± 1.7
1984	0.002 ± 0.005	0.7 ± 1.5	0.013 ± 0.008	0.5 ± 1.5	0.008 ± 0.007	0.6 ± 1.5
1985	0.003 ± 0.005	1.3 ± 1.7	0.013 ± 0.009	0.7 ± 0.9	0.008 ± 0.007	1.0 ± 1.3
1986	0.005 ± 0.006	1.9 ± 1.7	0.014 ± 0.009	0.9 ± 0.7	0.010 ± 0.008	1.4 ± 1.2
1987	0.007 ± 0.007	2.5 ± 1.5	0.015 ± 0.009	1.3 ± 0.9	0.011 ± 0.008	1.9 ± 1.2
1988	0.010 ± 0.008	3.1 ± 1.1	0.017 ± 0.008	1.6 ± 1.1	0.013 ± 0.008	2.3 ± 1.1
1989	0.013 ± 0.008	3.6 ± 0.7	0.019 ± 0.007	2.0 ± 1.2	0.016 ± 0.008	2.8 ± 1.0
1990	0.017 ± 0.008	4.1 ± 0.5	0.021 ± 0.006	2.3 ± 1.2	0.019 ± 0.007	3.2 ± 0.8
1991	0.021 ± 0.008	4.5 ± 0.5	0.023 ± 0.005	2.7 ± 1.2	0.022 ± 0.007	3.6 ± 0.8
1992	0.026 ± 0.008	4.8 ± 0.7	0.026 ± 0.004	3.0 ± 1.1	0.026 ± 0.006	3.9 ± 0.9
1993	0.031 ± 0.007	5.0 ± 0.9	0.029 ± 0.003	3.4 ± 0.9	0.030 ± 0.005	4.2 ± 0.9
1994	0.036 ± 0.007	5.1 ± 1.0	0.033 ± 0.002	3.8 ± 0.8	0.034 ± 0.004	4.4 ± 0.9
1995	0.041 ± 0.006	5.2 ± 1.0	0.037 ± 0.002	4.1 ± 0.6	0.039 ± 0.004	4.6 ± 0.8
1996	0.046 ± 0.005	5.1 ± 1.0	0.041 ± 0.002	4.4 ± 0.5	0.044 ± 0.003	4.8 ± 0.8
1997	0.051 ± 0.004	5.0 ± 1.0	0.045 ± 0.002	4.6 ± 0.4	0.048 ± 0.003	4.8 ± 0.7
1998	0.056 ± 0.003	4.8 ± 0.8	0.050 ± 0.002	4.8 ± 0.4	0.053 ± 0.002	4.8 ± 0.6
1999	0.061 ± 0.002	4.5 ± 0.7	0.055 ± 0.002	4.9 ± 0.4	0.058 ± 0.002	4.7 ± 0.6
2000	0.065 ± 0.002	4.2 ± 0.6	0.060 ± 0.002	4.9 ± 0.4	0.063 ± 0.002	4.5 ± 0.5
2001	0.069 ± 0.001	3.7 ± 0.5	0.065 ± 0.002	4.6 ± 0.4	0.067 ± 0.002	4.2 ± 0.4
2002	0.073 ± 0.001	3.2 ± 0.4	0.069 ± 0.002	4.2 ± 0.4	0.071 ± 0.002	3.7 ± 0.4
2003	0.076 ± 0.001	2.8 ± 0.4	0.073 ± 0.002	3.5 ± 0.4	0.074 ± 0.001	3.1 ± 0.4
2004	0.078 ± 0.001	2.3 ± 0.5	0.076 ± 0.001	2.9 ± 0.4	0.077 ± 0.001	2.6 ± 0.4
2005	0.081 ± 0.001	2.0 ± 0.6	0.079 ± 0.001	2.4 ± 0.4	0.080 ± 0.001	2.2 ± 0.5
2006	0.082 ± 0.002	1.6 ± 0.8	0.081 ± 0.001	2.0 ± 0.3	0.082 ± 0.002	1.8 ± 0.6
2007	0.084 ± 0.002	1.4 ± 1.0	0.083 ± 0.001	1.7 ± 0.3	0.083 ± 0.002	1.5 ± 0.7
2008	0.085 ± 0.003	1.2 ± 1.2	0.085 ± 0.001	1.4 ± 0.3	0.085 ± 0.002	1.3 ± 0.8
2009	0.086 ± 0.004	1.0 ± 1.2	0.086 ± 0.001	1.2 ± 0.4	0.086 ± 0.003	1.1 ± 0.8
2010	0.087 ± 0.006	1.0 ± 1.1	0.087 ± 0.001	1.0 ± 0.4	0.087 ± 0.003	1.0 ± 0.7
2011	0.088 ± 0.007	1.0 ± 0.7	0.088 ± 0.001	0.9 ± 0.4	0.088 ± 0.004	0.9 ± 0.6

* Annual hemispheric mean mole fractions and growth rates are estimated from the smoothing cubic spline fits.

the PFCs studied here at a globally averaged background tropospheric mole fraction of 0.27 ppt in 2011. The globally averaged atmospheric mole fraction in 2011 is 0.12 ppt for C_7F_{16}, and C_8F_{18} is the least abundant of all of these PFCs at 0.09 ppt. The growth rate of C_6F_{14} peaks in 1999 and has since declined to a 2011 annual global average of 5.0 ppq yr^{-1}. The trend in C_7F_{16}'s growth rates differ from the other PFCs, in that its growth has been relatively constant at 3 to 4 ppq yr^{-1} for the last 15 years. The atmospheric trends and growth rates of C_8F_{18} are similar to those of C_6F_{14}, although with lower absolute values, with a 2011 mean growth rate of 0.9 ppq yr^{-1}. As seen with C_4F_{10} and C_5F_{12}, the NH archived air samples for C_6F_{14}, C_7F_{16} and C_8F_{18} have higher atmospheric mole fractions than the SH samples with similar fill dates, suggesting that the emissions

are primarily in the NH. There is one NH sample with a fill date in 1986 with anomalously low values for C_6F_{14}, C_7F_{16} and C_8F_{18}, lower than the atmospheric mole fractions found in the SH samples with similar fill dates. However, this 1986 NH air sample is below the detection limit of the SIO instrument. Furthermore, this sample was not filled for the purpose of an air archive and has been shown to have depleted mole fractions for C_2F_6, C_3F_8 and sulfur hexafluoride (SF_6) most likely due to the fill technique. The absolute maximum growth rate is higher in the SH than in the NH for C_6F_{14} and C_8F_{18}. This is most likely a result of the lack of NH data in the 1990s to constrain the cubic smoothed spline fit and not that SH emissions dominate globally.

Recently Laube et al. (2012) also published atmospheric observations for C_4F_{10}, C_5F_{12}, C_6F_{14} and C_7F_{16}. Their
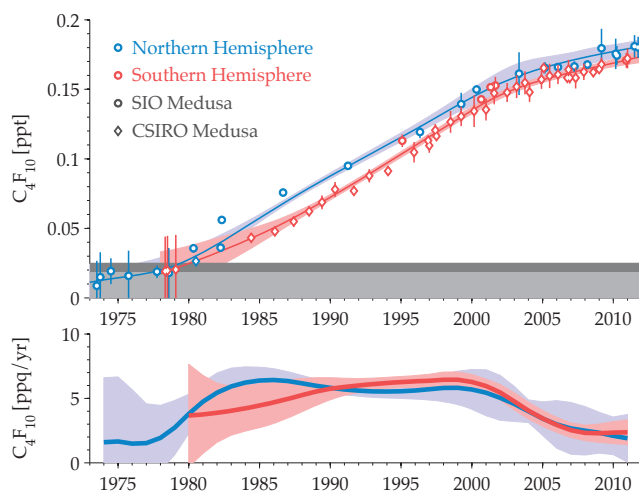
Fig. 1. The top panel shows the atmospheric mole fractions of C_4F_{10} based on Northern Hemisphere (blue circles and diamonds) and Southern Hemisphere (red circles and diamonds) archived air sample measurements. The circles are for the samples measured on the SIO Medusa and the diamonds are for the samples measured on the CSIRO Medusa. The vertical bars on the observations denote the 1-σ standard deviations of the sample measurements (often the measurement uncertainty is too small to be seen on the figure). The blue and red lines are the best fits to the Northern Hemisphere and Southern Hemisphere observations, respectively, and the shading is their estimated uncertainties. The grey shading shows the detection limits for the two Medusa systems, with light grey for the SIO Medusa and dark grey for the CSIRO Medusa. The bottom panel shows the average annual growth rates in mole fractions for the Northern (blue) and Southern (red) Hemispheres, calculated from the smoothing spline fits, and their estimated uncertainties, shown as the shading.
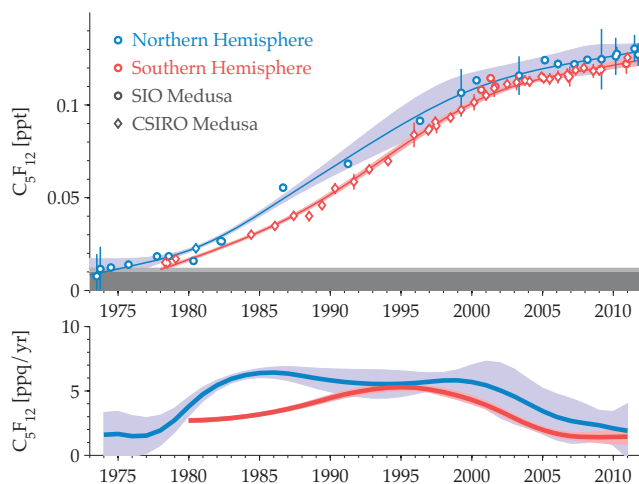
Fig. 2. Same as Fig. 1, but for C_5F_{12}.
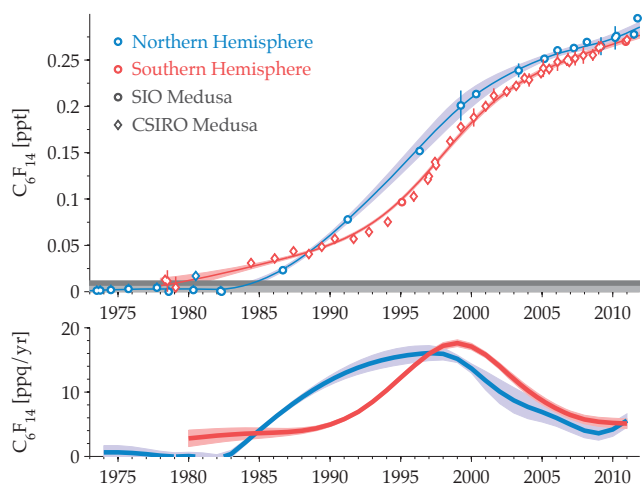
Fig. 3. Same as Fig. 1, but for C_6F_{14}.

results agree fairly with those presented here. The most notable differences are for C_5F_{12}, where Laube et al. (2012) reports a 2010 mole fraction that is 17 % higher than that presented here, and for C_7F_{16}, where Laube et al. (2012) finds a 2010 mole fraction that is 12 % lower than the estimate in this study. These differences most likely can be attributed to differences in calibration scales. In particular, the calibration scale estimated by Laube et al. (2012) for C_7F_{16} was prepared using an 85 % n-isomer of C_7F_{16} and may be a contributing factor to the differences between the two studies.

Based on the globally averaged 2011 atmospheric mole fractions (Tables 3-7), the global radiative forcing of each PFC can be estimated using the radiative efficiencies presented in Table 1. For C_4F_{10}, C_5F_{12} and C_6F_{14} we use the radiative efficiencies given by Forster et al. (2007), and for C_7F_{16} and C_8F_{18}, we use the radiative efficiencies given by Ivy et al. (2012). C_6F_{14} contributes the most of these high molecular weight PFCs to the global radiative forcing in 2011, and is similar to that of C_3F_8 (Mühle et al., 2010). The other PFCs in this study contribute approximately equally to global radiative forcing; and in total the high molecular weight PFCs 2011 atmospheric mole fractions contribute to a globally averaged radiative forcing of 0.35 mW m^{-2}.

5 Conclusions and future implications

Atmospheric histories and long-term growth trends have been presented for the high molecular weight PFCs: C_4F_{10}, C_5F_{12}, C_6F_{14}, C_7F_{16} and C_8F_{18}. These histories and trends are based on new measurements of a collection of NH archived air samples and a subset of the CGAA. The measurements were made with the Medusa systems and are calibrated against new primary standards for these PFCs. The contribution of all of the heavy PFCs studied here to global radiative forcing is 0.35 mW m^{-2}. While this is relatively small compared to the total radiative forcing of
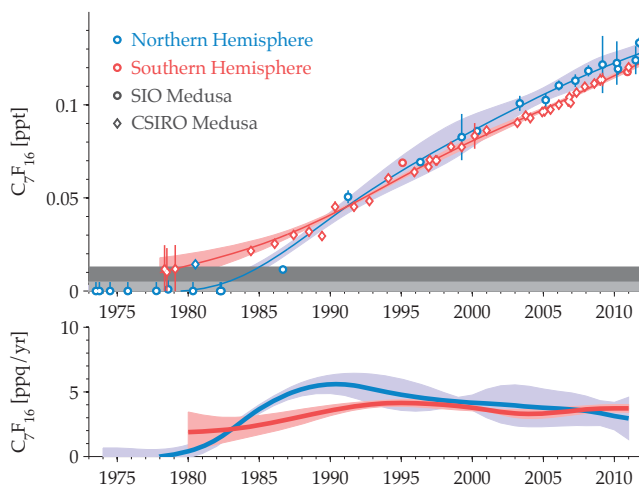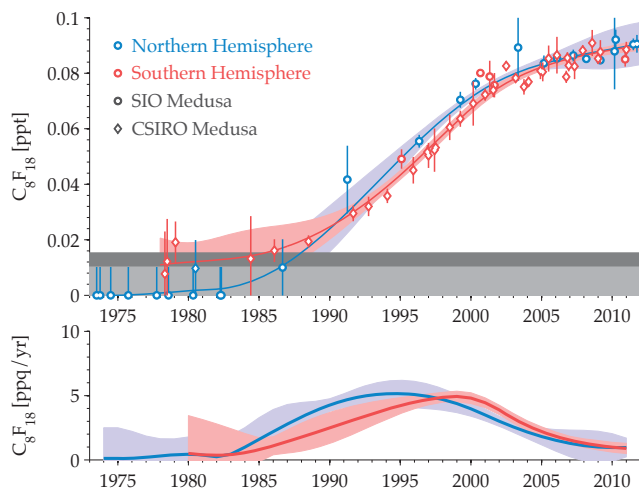
Fig. 4. Same as Fig. 1, but for C_7F_{16}.

Fig. 5. Same as Fig. 1, but for C_8F_{18}.

$2434 \, \text{mW m}^{-2}$ in 2008 for all species regulated under the Kyoto Protocol, the heavy PFC atmospheric mole fractions in 2011 contribute up to 6 % of the total anthropogenic PFC radiative forcing (Montzka and Reimann, 2011; Mühle et al., 2010; Oram et al., 2012).

The heavy PFCs in this study exhibited the largest growth rates in the 1980s and 1990s and have since slowed, suggesting that recent emissions may be decreasing as alternative compounds, with most likely lower GWPs, are used (Office of Air and Radiation and Office of Atmospheric Programs, 2006). Based on previous studies, atmospheric observations are crucial in providing measurement-based emission estimates to verify bottom-up inventories, which often show large discrepancies (Mühle et al., 2010; Oram et al., 2012). Additionally, future observations of these high molecular weight PFCs will be important in confirming that the semiconductor industry, which primarily focus on the use of low molecular weight PFCs, are indeed reducing global

PFC emissions (Semiconductor Industry Association, 2001; World Semiconductor Council, 2005). Although PFCs contribute a relatively small amount to global radiative forcing, due to their long lifetimes they are considered to have a permanent effect on the Earth's radiative budget when human timescales are considered.

Supplementary material related to this article is available online at: http://www.atmos-chem-phys.net/12/ 4313/2012/acp-12-4313-2012-supplement.pdf.

References

Arnold, T., Mühle, J., Salameh, P. K., Harth, C. M., Ivy, D. J., and Weiss, R. F.: Automated Measurement of Nitrogen Trifluoride in Ambient Air, Anal. Chem., in press, doi:10.1021/ac300373e, 2012.

Bravo, I. A., Aranda, A., Hurley, M. D., Marston, G., Nutt, D. R., Shine, K. P., Smith, K., and Wallington, T. J.: Infrared absorption spectra, radiative efficiencies, and global warming potentials of perfluorocarbons: comparison between experiment and theory, J. Geophys. Res., 115, D24317, doi:10.1029/2010JD014771, 2010.

Deeds, D. A., Vollmer, M. K., Kulongoski, J. T., Miller, B. R., Mühle, J., Harth, C. M., Izbicki, J. A., Hilton, D. R., and Weiss, R. F.: Evidence for crustal degassing of CF_4 and SF_6 in Mojave Desert groundwaters, Geochim. Cosmochi. Ac., 72(4), 999–1013, doi:10.1016/j.gca.2007.11.027, 2008.

Ellison, S. L. R. and Thompson, M.: Standard additions: myth and reality, The Analyst, 133, 992–997, doi:10.1039/b717660k, 2008.

Enting, I. G., Trudinger, C. M., and Etheridge, D. M.: Propagating data uncertainty through smoothing spline fits, Tellus B, 58, 305–309, doi:10.1111/j.1600-0889.2006.00193.x, 2006.

European Commission, Joint Research Centre (JRC)/Netherlands Environmental Assessment Agency (PBL): Emission Database

for Global Atmospheric Research (EDGAR), Release 4.0, available at: http://edgar.jrc.ec.europa.eu, last access: 15 December 2011, 2009.

Forster, P., Ramaswamy, V., Artaxo, P., Berntsen, T., Betts, R., Fahey, D. W., Haywood, J., Lean, J., Lowe, D. C., Myhre, G., Nganga, J., Prinn, R., Raga, G., Schulz, M., and Van Dorland, R.: Changes in atmospheric constituents and in radiative forcing, in: Climate Change 2007: The Physical Science Basis. Contribution of Working Group 1 to the Fourth Assessment Report of the Intergovernmental Panel on Climate Change, edited by: Solomon, S., Qin, D., Manning, M., Chen, Z., Marquis, M., Averyt, K. B., Tignor, K. B., and Miller, H. L., Cambridge Univ. Press, Cambridge, UK and New York, NY, USA, 2007.

Francey, R. J., Steele, L. P., Spencer, D. A., Langenfelds, R. L., Law, R. M., Krummel, P. B., Fraser, P. J., Etheridge, D. M., Derek, N., Coram, S. A., Cooper, L. N., Allison, C. E., Porter, L., and Baly, S.: The CSIRO (Australia) measurement of greenhouse gases in the global atmosphere, in: Baseline Atmospheric Program Australia 1999–2000, edited by: Tindale, N. W., Derek, N., and Fraser, P. J., Bur. of Meteorol., Melbourne, Victoria, Australia, 42–53, 2003.

Harnisch, J., Borchers, R., Fabian, P., Gäggeler, H. W., and Schotterer, U.: Effect of natural tetrafluoromethane, Nature, 384, p. 32, doi:10.1038/384032a0, 1996a.

Harnisch, J., Borchers, R., Fabian, P., and Maiss, M.: Tropospheric trends for CF_4 and C_2F_6 since 1982 derived from SF_6 dated stratospheric air, Geophys. Res. Lett., 23, 1099–1102, doi:10.1029/96GL01198, 1996b.

International Aluminium Institute: Results of the 2010 Anode Effect Survey: Report on the Aluminum Industry's Global Perfluorocarbon Gases Emissions Reduction Programme, International Aluminium Institute, London, UK, 2011.

Ivy, D. J., Rigby, M., Baasandorj, M., Burkholder, J. B., and Prinn, R. G.: Global emission estimates and radiative impact of the high molecular weight perfluorocarbons: C_4F_{10}, C_5F_{12}, C_6F_{14}, C_7F_{16} and C_8F_{18}, Atmos. Chem. Phys. Discuss., accepted, 2012.

Krummel, P. B., Langenfelds, R. L., Fraser, P. J., Steele, L. P., and Porter, L. W.: Archiving of Cape Grim air, in: Baseline Atmospheric Program (Australia) 2005–2006, edited by: Cainey, J. M., Derek, N., and Krummel, P. B., Bur. of Meteorol., Melbourne, Victoria, Australia, 55–57, 2007.

Langenfelds, R. L., Fraser, P. J., Francey, R. J., Steele, L. P., Porter, L. W., and Allison, C. E.: The Cape Grim air archive: the first seventeen years, 1978–1995, in: Baseline Atmospheric Program (Australia) 1994–1995, edited by: Francey, R. J., Dick, A. L., and Derek, N., Bur. of Meteorol., Melbourne, Victoria, Australia, 53–70, 1996.

Laube, J. C., Hogan, C., Newland, M. J., Mani, F. S., Fraser, P. J., Brenninkmeijer, C. A. M., Martinerie, P., Oram, D. E., Röckmann, T., Schwander, J., Witrant, E., Mills, G. P., Reeves, C. E., and Sturges, W. T.: Distributions, long term trends and emissions of four perfluorocarbons in remote parts of the atmosphere and firn air, Atmos. Chem. Phys., 12, 4081–4090, doi:10.5194/acp-12-4081-2012, 2012.

Miller, B. R., Weiss, R. F., Salameh, P. K., Tanhua, T., Greally, B. R., Mühle, J., and Simmonds, P. G.: Medusa: a sample preconcentration and GC/MS detector system for in situ measurements of atmospheric trace halocarbons, hydrocarbons, and sulfur compounds, Anal. Chem., 80, 1536–1545, doi:10.1021/ac702084k, 2008.

Montzka, S. A. and Reimann, S.: Ozone-depleting substances (ODSs) and related chemicals, in: Scientific Assessment of Ozone Depletion: 2010, Global Ozone Research and Monitoring Project, Rep. 52, World Meteorol. Org., Geneva, Switzerland, 1–108, 2011.

Mühle, J., Ganesan, A. L., Miller, B. R., Salameh, P. K., Harth, C. M., Greally, B. R., Rigby, M., Porter, L. W., Steele, L. P., Trudinger, C. M., Krummel, P. B., O'Doherty, S., Fraser, P. J., Simmonds, P. G., Prinn, R. G., and Weiss, R. F.: Perfluorocarbons in the global atmosphere: tetrafluoromethane, hexafluoroethane, and octafluoropropane, Atmos. Chem. Phys., 10, 5145–5164, doi:10.5194/acp-10-5145-2010, 2010.

NIST Mass Spec Data Center, Stein, S. E., Director: Mass Spectra, in: NIST Chemistry WebBook, NIST Standard Reference Database Number 69, edited by: Linstrom, P. J. and Mallard, W. G., National Institute of Standards and Technology, Gaithersburg, Maryland, USA, http://webbook.nist.gov, (retrieved 9 October 2009).

Oram, D. E., Mani, F. S., Laube, J. C., Newland, M. J., Reeves, C. E., Sturges, W. T., Penkett, S. A., Brenninkmeijer, C. A. M., Röckmann, T., and Fraser, P. J.: Long-term tropospheric trend of octafluorocyclobutane (c-C_4F_8 or PFC-318), Atmos. Chem. Phys., 12, 261–269, doi:10.5194/acp-12-261-2012, 2012.

Office of Air and Radiation and Office of Atmospheric Programs, Climate Change Division: Uses and Emissions of Liquid PFC Heat Transfer Fluids from the Electronics Sector, in: US EPA Report EPA-430-R-06-901, United States Environmental Protection Agency, 2006.

Prinn, R. G., Weiss, R. F., Fraser, P. J., Simmonds, P. G., Cunnold, D. M., Alyea, F. N., O'Doherty, S., Salameh, P., Miller, B. R., Huang, J., Wang, R. H. J., Hartley, D. E., Harth, C., Steele, L. P., Sturrock, G., Midgley, P. M., and McCulloch, A.: A history of chemically and radiatively important gases in air deduced from ALE/GAGE/AGAGE, J. Geophys. Res., 105, 17751–17792, 2000.

Ravishankara, A. R., Solomon, S., Turnipseed, A. A., and Warren, R. F.: Atmospheric lifetimes of long-lived halogenated species, Science, 259, 194–199, doi:10.1126/science.259.5092.194, 1993.

Saito, T., Yokouchi, Y., Stohl, A., Taguchi, S., and Mukai, H.: Large emissions of perfluorocarbons in East Asia deduced from continuous atmospheric measurements, Environ. Sci. Technol., 44, 4089–4095, doi:10.1021/es1001488, 2010.

Semiconductor Industry Association: Semiconductor Industry Association Announces PFC Reduction and Climate Partnership with US EPA, Semiconductor Industry Association Press Release, 2001.

Shine, K. P., Gohar, L. K., Hurley, M. D., Marston, G., Martin, D., Simmonds, P. G., Wallington, T. J., and Watkins, M.: Perfluorodecalin: global warming potential and first detection in the atmosphere, Atmos. Environ., 39, 1759–1763, doi:10.1016/j.atmosenv.2005.01.001, 2005.

Tsai, W.: Environmental hazards and health risk of common liquid perfluoro-n-alkanes, potent greenhouse gases, Environ. Int., 35, 418–424, doi:10.1016/j.envint.2008.08.009, 2009.

Tuma, P. and Tousignant, L.: Reducing emissions of PFC heat transfer fluids, presented at SEMI Technical Symposium, 3M Specialty Materials, 1–8, San Francisco, CA, USA, 16 July 2001.

UNEP Technology and Economic Assessment Panel: The implications to the Montreal Protocol of the inclusion of HFCs and PFCs in the Kyoto Protocol, in: Report of the TEAP HFC and PFC Task Force, Ozone Secretariat, United Nations Environment Programme, Nairobi, Kenya 1–86, 1999.

World Semiconductor Council: Semiconductor manufacturers reduce PFC emissions, World Semiconductor Council Press Release, 2005.

Joint Program Reprints are available free of charge (limited quantities). To order: please use contact information on inside of front cover.

2012-31 Green growth and the efficient use of natural resources, Reilly, J.M., *Energy Economics*, 34(S1): S–S93 (2012)

2012-32 The role of China in mitigating climate change, Paltsev, S., J. Morris, Y. Cai, V. Karplus and H.D. Jacoby, *Energy Economics*, 34(S3): S444–S450 (2012)

2012-33 Valuing climate impacts in integrated assessment models: the MIT IGSM, John Reilly, Sergey Paltsev, Ken Strzepek, Noelle E. Selin, Yongxia Cai, Kyung-Min Nam, Erwan Monier, Stephanie Dutkiewicz, Jeffery Scott, Mort Webster and Andrei Sokolov, *Climatic Change*, online first, doi:10.1007/s10584-012-0635-x (2012)

2012-34 From "Green Growth" to sound policies: An overview, Schmalensee, Richard, *Energy Economics*, 34: S–S6 (2012)

2012-35 Shale gas production: potential versus actual greenhouse gas emissions, O'Sullivan, F. and S. Paltsev, *Environmental Research Letters*, 7(4): 044030 (2012)

2012-36 Atmospheric histories and growth trends of C_4F_{10}, C_5F_{12}, C_6F_{14}, C_7F_{16}, C_8F_{18}, Ivy, D.J., T. Arnold, C.M. Harth, L.P. Steele, J. Mühle, M. Rigby, P.K. Salameh, M. Leist, P.B. Krummel, P.J. Fraser, R.F. Weiss and R.G. Prinn, *Atmospheric Chemistry and Physics*, 12: 4313–4325 (2012)

2013-1 The Impact of Climate Policy on US Aviation, Winchester, Niven, Christoph Wollersheim, Regina Clewlow, Nicholas C. Jost, Sergey Paltsev, John M. Reilly and Ian A. Waitz, *Journal of Transport Economics and Policy*, 47(1): 1–15 (2013)

2013-2 Impact of anthropogenic absorbing aerosols on clouds and precipitation: A review of recent progresses, Wang, Chien, *Atmoshperic Research*, 122: 237–249 (2013)

2013-3 Applying engineering and fleet detail to represent passenger vehicle transport in a computable general equilibrium model, Karplus, Valerie, Sergey Paltsev, Mustafa Babiker and John M. Reilly, *Economic Modelling,* 30: 295–305 (2013)

2013-4 Should a vehicle fuel economy standard be combined with an economy-wide greenhouse gas emissions constraint? Implications for energy and climate policy in the United States, Karplus, Valerie, Sergey Paltsev, Mustafa Babiker and John M. Reilly, *Energy Economics*, 36: 322–333 (2013)

2013-5 Climate impacts of a large-scale biofuels expansion, Hallgren, W., C.A. Schlosser, E. Monier, D. Kicklighter, A. Sokolov and J. Melillo, *Geophysical Research Letters*, 40(8): 1624–1630 (2013)

2013-6 Non-nuclear, low-carbon, or both? The case of Taiwan, Chen, Y.-H.H., *Energy Economics*, 39: 53–65 (2013)

2013-7 The Cost of Adapting to Climate Change in Ethiopia: Sector-Wise and Macro-Economic Estimates, Robinson, S., K. Strzepek and Raffaello Cervigni, *IFPRI ESSP WP 53* (2013)

2013-8 Historical and Idealized climate model experiments: an intercomparison of Earth system models of intermediate complexity, Eby, M., A.J. Weaver, K. Alexander, K. Zickfield, A. Abe-Ouchi, A.A. Cimatoribus, E. Crespin, S.S. Drijfhout, N.R. Edwards, A.V. Eliseev, G. Feulner, T. Fichefet, C.E. Forest, H. Goosse, P.B. Holden, F. Joos, M. Kawamiya, D. Kicklighter, H. Kiernert, M. Matsumoto, I.I. Mokov, E. Monier, S.M. Olsen, J.O.P. Pedersen, M. Perrette, G. Phillpon-Berthier, A. Ridgwell, A Schlosser, T. Schneider von Deimling, G. Shaffer, R.S. Smith, R. Spahni, A.P. Sokolov, M. Steinacher, K. Tachiiri, K. Tokos, M. Yoshimori, N Zeng and F. Zhao, *Clim. Past*, 9:1111–1140 (2013)

2013-9 Correction to "Sensitivity of distributions of climate system properties to the surface temperature data set", and Sensitivity of distributions of climate system properties to the surface temperature data set, Libardoni, A.G. and C.E. Forest, *Geophysical Research Letters*, 40(10): 2309–2311 (2013), and 38(22): 1–6 (2011)

2013-10 Permafrost degradation and methane: low risk of biogeochemical climate-warming feedback, Gao, Xiang, C. Adam Schlosser, Andrei Sokolov, Katey Walter Anthony, Qianlai Zhuang and David Kicklighter, *Environmental Research Letters*, 8(3): 035014 (2013)

For a complete list of titles see:
http://globalchange.mit.edu/research/publications/reprints